Numerical Methods in Civil Engineering, 10-1 (2025) 31-45

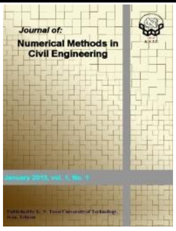

Numerical Methods in Civil Engineering

Journal Homepage: https://nmce.kntu.ac.ir/

Review and improvement of unloading and reloading stress-strain models for FRP-confined concrete

Amirhosein Raisszadeh*, Hadi Ziaadiny, Ehsan Khojastehfar*****

ARTICLE INFO

RESEARCH PAPER

Article history:
Received:
May 2025
Revised:
July 2025
Accepted:
August 2025

Keywords:
FRP,
Confinement,
Concrete column,
Cyclic behavior,
Stress-strain model

Abstract:

The cyclic stress-strain behavior of FRP-confined concrete columns is a key aspect of their performance, particularly in the context of seismic retrofitting and design. Significant research has been conducted in recent years to study the cyclic response of FRP-confined concrete in both circular and rectangular columns subjected to unloading and reloading cycles. These studies have led to the development of various cyclic stress-strain models to predict the behavior of FRP-confined concrete columns under such loading conditions.
However, critical gaps remain in the modeling of early-stage unloading strains, reloading slope reduction, and cross-section-dependent behavior. This paper begins by introducing the fundamental components of cyclic stress-strain behavior. Moreover, the text reviews and evaluates the existing models proposed for each aspect of this behavior, focusing on comparing their predictions with experimental data. Furthermore, modifications are suggested for components of the cyclic models that exhibit discrepancies when validated against experimental observations. These include a proposed reloading slope factor and refined unloading path formulations. These improvements aim to enhance the accuracy and reliability of cyclic stress-strain models for FRP-confined concrete columns, contributing to their effective application in structural design and seismic resilience.

1. Introduction

The cyclic stress-strain behavior of FRP-confined concrete columns plays a critical role in understanding their performance under seismic loading. This behavior is particularly significant for the seismic retrofitting and design of structural members, where FRP confinement is used to enhance ductility and strength. Over the past few decades, extensive research has been carried out to examine the cyclic behavior of FRP-confined concrete, with a focus on understanding its response to unloading and reloading cycles [1-4]. These investigations have aimed to provide insights into different aspects of cyclic behavior, including the envelope curve, plastic strain accumulation, stress deterioration, the impact of repeated loading cycles, and the effects of partial unloading and reloading cycles. Such studies are vital for the development of reliable cyclic stress-strain models that can predict the performance of FRP-confined concrete columns under various loading conditions. Recent advancements in FRP applications for seismic rehabilitation, including hybrid NSM-CFRP systems [5] and optimized FRP strip configurations [6, 7], have further demonstrated the material's versatility in structural applications. The models evaluated in this study were selected based on their widespread acceptance, demonstrated accuracy across diverse cross-sectional geometries and concrete strengths, and their ability to capture key behavioral features such as unloading/reloading paths and plastic strain accumulation. This selective approach ensures a balanced assessment of established models while identifying critical gaps in current predictive capabilities. Shao et al. [8] conducted a detailed experimental study involving 24 CFRP- and GFRP-wrapped circular concrete prisms subjected to complete and partial unloading-reloading cycles. The prisms, with dimensions of

* *Assistant Professor, Vali-e-Asr University of Rafsanjan, Rafsanjan, Iran. Email: a.raisszadeh@vru.ac.ir*

***Assistant Professor, Vali-e-Asr University of Rafsanjan, Rafsanjan, Iran. Email: h.ziaadiny@vru.ac.ir*

**** Corresponding author: Assistant Professor, Vali-e-Asr University of Rafsanjan, Rafsanjan, Iran. Email: e.khojastehfar@vru.ac.ir*

https://doi.org/10.61882/NMCE.2505.1090

152 mm in diameter and 305 mm in height, were fabricated using concrete with a 28-day compressive strength of 40 MPa. Their findings highlighted the influence of FRP confinement on cyclic stress-strain behavior, particularly on the unloading and reloading paths. Similarly, Lam et al. [9] tested 18 CFRP-confined concrete cylinders of identical dimensions under complete unloading-reloading cycles, understanding cyclic compression behavior in FRP-confined concrete. Based on these experimental observations, Lam and Teng [10] proposed a cyclic stress-strain model for FRP-confined circular concrete prisms, which became a foundational reference in this field.

Wang et al. [11] extended this work by examining both monotonic and cyclic behavior in large-scale CFRP-confined concrete columns, including unreinforced and reinforced (RC) circular columns. Their study revealed how confinement from CFRP wraps and internal steel reinforcement impacts stress-strain behavior, including parameters such as peak compressive stress, strain at failure, unloading/reloading paths, and plastic strain accumulation. Using their experimental data, Wang et al. proposed a cyclic stress-strain model for CFRP-confined circular RC columns. Additionally, Wang et al. [12] investigated CFRP-confined square RC columns under both monotonic and cyclic loading. In their subsequent work, they introduced a cyclic stress-strain model for square RC columns, addressing specific aspects of their cyclic behavior and confinement effects.

Yu et al. [13] reviewed Lam and Teng's model [10] and identified limitations stemming from the small dataset available to the original authors. They developed an improved cyclic stress-strain model to address these deficiencies, ensuring its applicability to both normal-strength concrete (NSC) and high-strength concrete (HSC) confined with FRP wraps or placed in concrete-filled FRP tubes (CFFTs). This model offered improved predictions for cyclic behavior across various conditions. Ziaadiny and Abbasnia [14], according to the results of an extensive series of cyclic compressive loading tests, proposed a unified cyclic stress-strain model for FRP-confined columns of circular, square, and rectangular cross-sections. Their model provided a comprehensive framework that incorporated different components of the cyclic stress-strain curve, including new formulations for unloading and reloading paths, thereby improving the predictive capabilities of existing models.

Despite these advancements, existing cyclic stress-strain models often fail to account for certain critical parameters influencing the behavior of FRP-confined concrete columns, such as loading history, partial unloading/reloading effects, and stress deterioration under repeated cycles. These gaps in the models limit their accuracy and generalizability, especially when applied to diverse structural conditions. Addressing these limitations is essential to improve the reliability of cyclic models for practical applications in structural design and seismic retrofitting.

In this paper, a comprehensive review of different components of cyclic stress-strain behavior is presented, focusing on envelope curves, plastic strain, stress deterioration, and the effects of repeated and partial unloading/reloading cycles. The performance of existing cyclic models is evaluated through comparisons with experimental results, and a critical assessment of their limitations is provided. Based on these findings, modifications to current models are proposed to enhance their accuracy and applicability. These improvements are expected to contribute to the development of more robust cyclic stress-strain models, which are essential for designing safer and more resilient structures under cyclic loading conditions.

2. Monotonic stress-strain models for envelope curve

Studies on unconfined, steel-confined, and FRP-confined concrete have consistently demonstrated that the envelope curve of cyclic stress-strain behavior corresponds closely to the monotonic stress-strain curve for the same type of concrete under monotonic loading conditions. This alignment highlights the applicability of monotonic stress-strain models for predicting the envelope curve in cyclic behavior, emphasizing their importance in understanding and modeling FRP-confined concrete under complex loading scenarios. Consequently, accurate and reliable monotonic stress-strain models developed for FRP-confined concrete prisms have become a foundational basis for representing the cyclic envelope curve.

Shao et al. [8] in their investigation, employed the monotonic stress-strain model proposed by Samaan et al. [15] for FRP-confined concrete to estimate the envelope curve of cyclic stress-strain behavior. Their findings demonstrated the validity of utilizing monotonic models for this purpose and underscored the versatility of Samaan et al.'s model in representing cyclic behavior. Similarly, Lam and Teng [10] conducted a range of experimental and analytical studies to confirm that the monotonic stress-strain model they developed [16] is capable of accurately predicting the envelope curves for their FRP-confined concrete specimens. Based on their results, Lam and Teng [10] incorporated their monotonic model into the modeling of the cyclic stress-strain envelope, further establishing its robustness and reliability.

Expanding the scope of research to FRP-confined rectangular prisms, Abbasnia et al. [17-22] investigated specimens with varying confinement levels, aspect ratios, corner radius, and concrete strengths. Their study revealed that, for these specimens, the monotonic stress-strain curve serves as a tangent to the upper boundary of the cyclic stress-strain curve, reinforcing the relationship between monotonic and cyclic behavior. However, Abbasnia and Ziaadiny [23], after assessing several existing monotonic stress-strain models for rectangular columns, identified notable deficiencies in their predictive capabilities. They concluded that none of the assessed models could accurately predict the stress and strain at the ultimate point, particularly under conditions where the aspect ratio significantly influences the ultimate behavior. This limitation was seen as a critical gap in the applicability of monotonic models, requiring further refinement to enhance their accuracy.

Based on these advancements, Yu et al. [13] adopted an enhanced version of the Lam and Teng model [16], which was subsequently refined by Teng et al. [24]. This refined model introduced more accurate formulations for key parameters, including the ultimate axial strain and compressive strength, thereby significantly improving the predictive accuracy of the envelope stress-strain curves for FRP-confined concrete. The refined model demonstrated its versatility by applying to concrete-filled FRP tubes (CFFTs) as well as FRP-wrapped concrete, effectively covering a wider range of confinement scenarios. By addressing the limitations of earlier models, this refined approach provided a more comprehensive framework for modeling the cyclic envelope curve, further advancing the understanding of FRP-confined concrete behavior.

3. Residual strain for the first cycle

The residual axial strain of concrete upon unloading to zero stress is referred to as plastic strain [19]. This parameter is fundamental in modeling the behavior of concrete during unloading and reloading cycles. Research on steel-confined and FRP-confined concrete has demonstrated a linear relationship between the plastic strain in the first unloading/reloading cycle, $\varepsilon_{pl,1}$, and the strain at the point where unloading begins from the envelope curve, $\varepsilon_{ul,1}$. While empirical relationships effectively capture plastic strain behavior in conventional cases, their theoretical basis for high-strength concretes and non-circular sections requires further mechanistic justification - a gap addressed through our proposed modifications by correlating R^2 improvements with confinement effectiveness across section geometries.

Several models have been proposed for predicting plastic strain, and these are summarized below:

3.1 Shao et. al.'s model [8] for circular prisms

Shao et al. proposed the following equation for plastic strain in the envelope cycles:

$$\varepsilon_{pl,1} = \varepsilon_{ul,1} - \frac{f_{ul,1}}{E_{sec\,u}} \tag{1}$$

Where $E_{sec\,u}$ is the unloading modulus defined as:

$$\frac{E_{sec\,u}}{E_c} = \begin{cases} 1 & 0 \le \frac{f_{ul,1}}{f'_{co}} < 1 \\ -0.44\frac{f_{ul,1}}{f'_{co}} + 1.44 & 1 \le \frac{f_{ul,1}}{f'_{co}} < 2.5 \\ 0.34 & \frac{f_{ul,1}}{f'_{co}} \ge 2.5 \end{cases} \tag{2}$$

Where the elastic modulus of unconfined concrete is

$$E_c = 3950\sqrt{f'_{co}} \quad (MPa)$$

3.2 Lam and Teng's model [10] for circular prisms

Lam and Teng [10] suggested that for FRP-confined concrete prisms $\varepsilon_{pl,1} = 0$if $\varepsilon_{ul,1} \le 0.001$. They also illustrated that for $\varepsilon_{ul,1} > 0.001$ the plastic strain $\varepsilon_{pl,1}$ is a linear function of the envelope unloading strain $\varepsilon_{ul,1}$, and proposed two different equations for the interval between unloading strain ranges less than 0.0035 and greater than 0.0035:

$$\varepsilon_{pl,1} = \begin{cases} 0, & 0 < \varepsilon_{ul,1} \le 0.001 \\ \left[1.4\left(0.87 - 0.004f'_{co}\right) - 0.64\right] \times (\varepsilon_{ul,1} - 0.001), & 0.001 < \varepsilon_{ul,1} < 0.0035 \\ (0.87 - 0.004f'_{co})\varepsilon_{ul,1} - 0.0016, & \varepsilon_{ul,1} \ge 0.0035 \end{cases} \tag{3}$$

3.3 Yu et al.'s model [13] for circular prisms

Yu et al. [13] assessed Lam and Teng's model [10] based on their tests on concrete-filled FRP tubes and FRP confined concrete specimens. They also examined the cyclic behavior of normal and high-strength concrete confined with FRP wrap. They proposed the following linear equation for the envelope plastic strain of FRP-confined concrete.

$$\varepsilon_{pl,1} = \begin{cases} 0, & 0 < \varepsilon_{ul,1} \le 0.001 \\ 0.184\varepsilon_{ul,1} - 0.0002, & 0.001 < \varepsilon_{ul,1} \le 0.0035 \\ 0.703\varepsilon_{ul,1} - 0.002, & \varepsilon_{ul,1} > 0.0035 \end{cases} \tag{4}$$

This relationship shows that, unlike the above-mentioned models the plastic strain in Yu et al.'s model [13] depends only on the envelope unloading strain.

3.4 Ziaadiny and Abbasnia's model [14] for square, rectangular, and circular prisms

Abbasnia et al. [17-21] examined how various factors, including confinement level, aspect ratio, corner radius, and concrete strength, influence the plastic strain of FRP-confined rectangular prisms. Their findings indicated that

plastic strain is primarily determined by the concrete strength. In a related study, Ziaadiny and Abbasnia [14] observed that circular specimens exhibit lower plastic strain compared to square and rectangular prisms. They proposed specific equations to estimate the plastic strain for both cylindrical and rectangular specimens.
For cylindrical specimens:

$$\varepsilon_{pl,1} = \begin{cases} 0, & 0 \le \varepsilon_{ul,1} < 0.001 \\ [1.4(0.800 - 0.0047f'_{co}) - 0.6] \times (\varepsilon_{ul,1} - 0.001), & 0.001 \le \varepsilon_{ul,1} < 0.0035 \\ (0.800 - 0.0047f'_{co})\varepsilon_{ul,1} - 0.001, & \varepsilon_{ul,1} \ge 0.0035 \end{cases} \quad (5\text{-a})$$

For rectangular specimens:

$$\varepsilon_{pl,1} = \begin{cases} 0, & 0 \le \varepsilon_{ul,1} < 0.001 \\ [1.4(0.856 - 0.0046f'_{co}) - 0.56] \times (\varepsilon_{ul,1} - 0.001), & 0.001 \le \varepsilon_{ul,1} < 0.0035 \\ (0.856 - 0.0046f'_{co})\varepsilon_{ul,1} - 0.0014, & \varepsilon_{ul,1} \ge 0.0035 \end{cases} \quad (5\text{-b})$$

Where f'_{co} is the unconfined concrete strength in MPa.
Figure 1 compares experimental plastic strains in circular specimens with predictions from various analytical models. Since unconfined concrete strength is the dominant parameter affecting plastic strain, specimens with varying strengths were selected for evaluation. It is evident from these figures that plastic strain is reduced by increasing unconfined concrete strength, thus the models that consider this effect can provide better predictions for plastic strain. Generally, Lam and Teng's model [10] has better predictions for the plastic strain. Shao et al.'s model tends to overestimates the plastic strains particularly for concrete with lower strength. Yu et al. [13] did not consider the effect of concrete strength, thus their model has some errors for higher-strength concretes. Ziaadiny and Abbasnia's formulation provides relatively good predictions for plastic strain but lacks accuracy for higher-strength concrete. Thus, the model of Lam and Teng [10] is recommended for the prediction of the plastic strain of FRP-confined concrete.

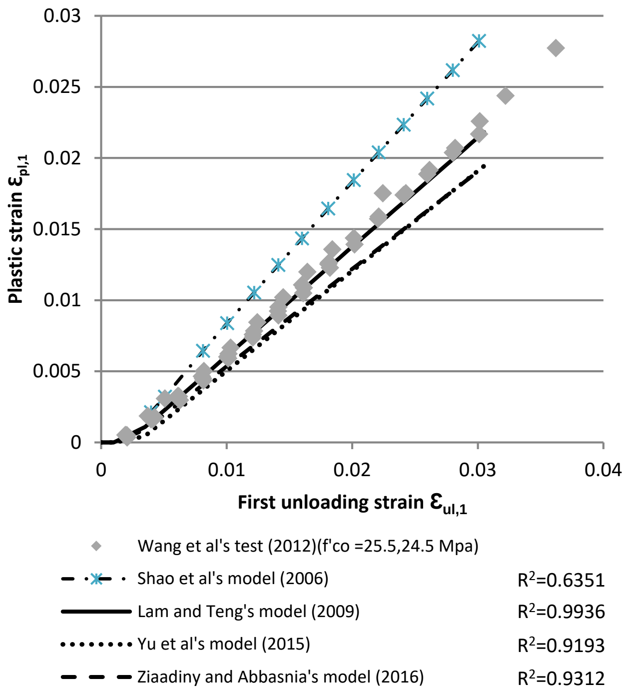

(a)

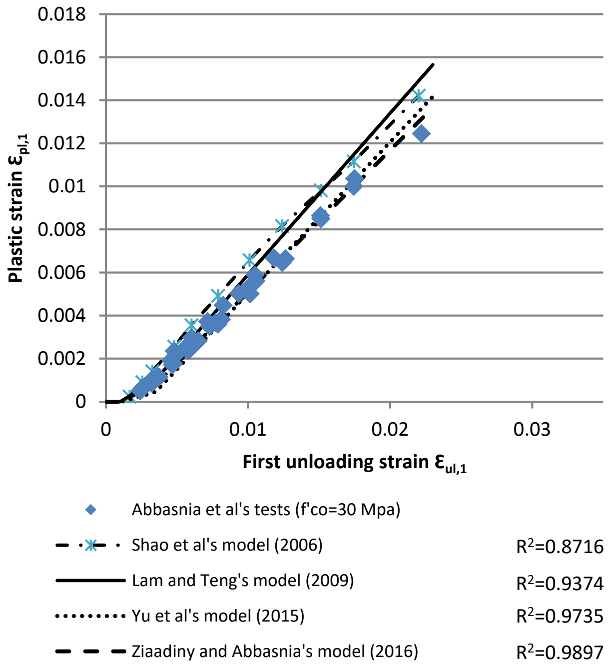

(b)

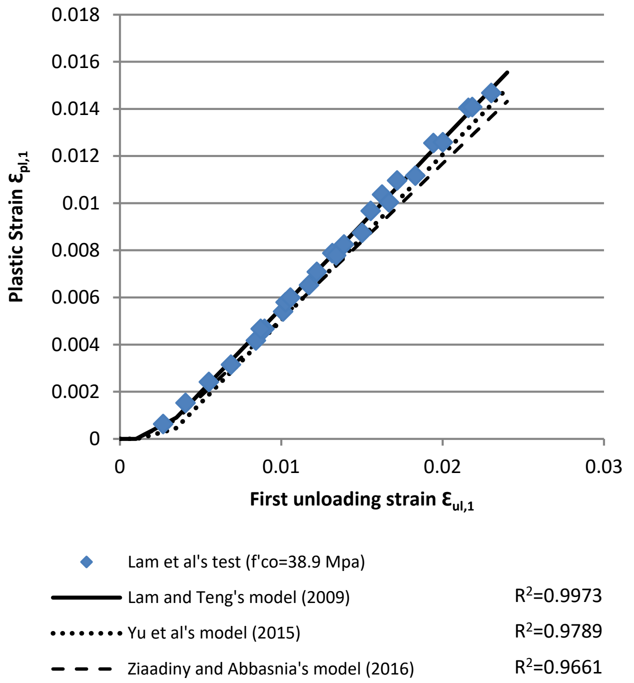

(c)

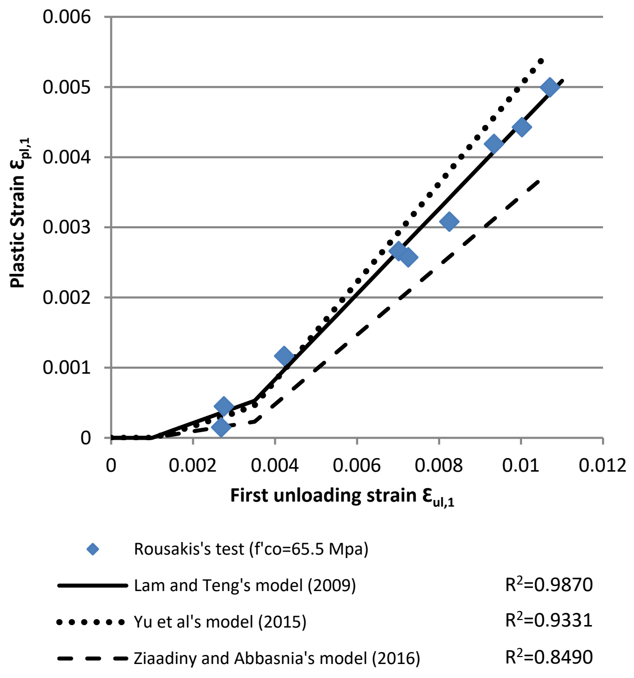

(d)

Fig. 1: Plastic strain in circular specimens versus model predictions: **a)** Experimental specimen: Wang et al.'s test ($f'_{co} = 25.5, 24.5\ MPa$), **b)** Experimental specimen: Abbasnia et al.'s test ($f'_{co} = 30\ MPa$), **c)** Experimental specimen: Lam et al.'s test ($f'_{co} = 38.9\ MPa$), **d)** Experimental specimen: Rousakis's test ($f'_{co} = 65.5\ MPa$)

4. Stress deterioration of envelope cycles

The cyclic behavior of FRP-confined concrete, as shown in various studies indicates that unloading and reloading cycles result in strength degradation. Following an unloading/reloading cycle, the concrete does not regain the envelope unloading stress at the corresponding envelope unloading strain but instead reaches a lower stress level, denoted as $f_{new,1}$.

To assess this strength reduction, most cyclic stress-strain models introduce a stress deterioration ratio. This parameter quantifies the degree of stress loss during the first unloading/reloading path of each cycle, offering a critical measure for understanding and modeling the progressive weakening of FRP-confined concrete under cyclic loading.

$$\beta_1 = \frac{f_{new,1}}{f_{ul,1}} \tag{6}$$

Shao et al. [8] proposed the constant value of 0.9 for β_1, But Lam and Teng, Yu et al., and Ziaadiny and Abbasnia [10, 13, 14] proposed variable formulations for β_1 as follows:

Lam and Teng's model [10] for circular prisms:

$$\beta_1 = \begin{cases} 1, & 0 \le \varepsilon_{ul,1} < 0.001 \\ 1 - 80(\varepsilon_{ul,1} - 0.001), & 0.001 \le \varepsilon_{ul,1} < 0.002 \\ 0.92, & \varepsilon_{ul,1} \ge 0.002 \end{cases} \tag{7}$$

Yu et al.'s model [13] for circular prisms:

$$\beta_1 = \begin{cases} 1, & 0 \le \varepsilon_{ul,1} < 0.001 \\ 1 - 32(\varepsilon_{ul,1} - 0.001), & 0.001 \le \varepsilon_{ul,1} < 0.0035 \\ 0.92, & \varepsilon_{ul,1} \ge 0.0035 \end{cases} \tag{8}$$

Ziaadiny and Abbasnia's model [14] for square, rectangular, and circular prisms:

$$\beta_1 = \left\{ \begin{matrix} 1 & 0 \le \varepsilon_{ul,1} < 0.001 \\ -40\varepsilon_{ul,1} + 1.04 & 0.001 \le \varepsilon_{ul,1} < 0.0035 \\ 0.9 & \varepsilon_{ul,1} \ge 0.0035 \end{matrix} \right\} \tag{9}$$

Figure 2 depicts the stress deterioration ratio versus different envelope unloading strains from experimental results. Specimens with different characteristics are chosen to involve all parameters that can affect the stress deterioration ratio. It is evident from this figure that stress deterioration for the early unloading strains is low and with the increase of unloading strain trends to a constant value. For the unloading strain less than 0.0035, only Shao et al.'s model makes no reasonable predictions. For unloading strain greater than 0.0035, Shao et al.'s model and Ziaadiny and Abbasnia's model are 0.9 for β_1, and Lam and Teng's model and Yu et al.'s model are 0.92. From the all-experimental results, the average value of β_1 for unloading strains greater than 0.0035, is obtained as 0.907. Thus, it is recommended that for $\varepsilon_{ul,env} \geq 0.0035$ stress deterioration ratio β_1 to be taken as 0.91.

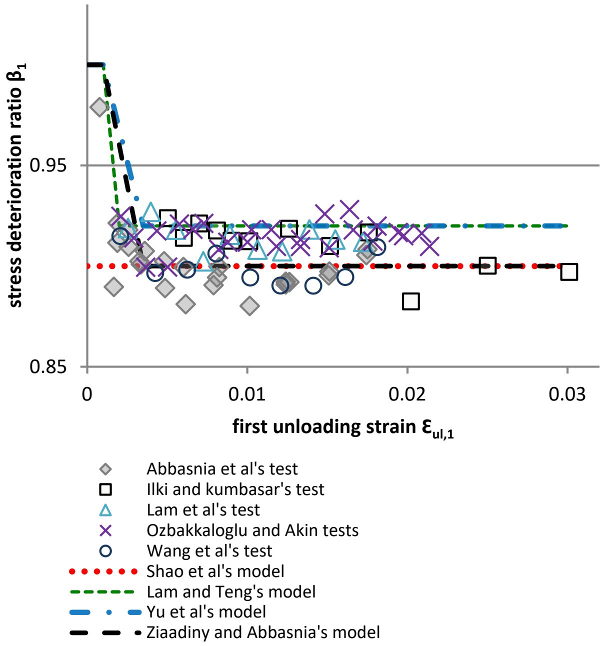

Fig. 2: Correlations between β_1 and $\varepsilon_{ul,1}$ for the specimens with different characteristics and the predictions of models

5. Loading history and effect of repeated cycles

Several studies have investigated the cyclic behavior of unconfined and confined concrete, particularly focusing on the effects of repeated complete unloading and reloading cycles. Shao et al. [8] in their research on FRP-confined concrete cylinders, introduced the concept of uniqueness, suggesting that repeated unloading/reloading cycles follow identical paths in FRP-confined concrete. However, subsequent studies have challenged this notion, arguing that the uniqueness concept does not hold for FRP-confined concrete. Instead, these studies highlight that loading history has a cumulative impact, contributing to the progressive accumulation of plastic strain and stress deterioration [17, 20-22].

In response to these findings, several researchers have developed formulations to model and predict the effects of repeated unloading/reloading cycles. These formulations aim to capture the cumulative changes in plastic strain and stress levels, offering improved accuracy for cyclic stress-strain models of FRP-confined concrete.

5.1 Plastic strain of repeated complete cycles

In most studies on cyclic behavior, the impact of repeated complete unloading/reloading cycles on plastic strain is assessed using the increasing strain ratio, γ_n, originally introduced by Sakai and Kawashima [25]. The ratio is defined as:

$$\gamma_n = \frac{\varepsilon_{ul,1} - \varepsilon_{pl,n}}{\varepsilon_{ul,1} - \varepsilon_{pl,n-1}} \tag{10}$$

Here, $\varepsilon_{pl,n}$ represents the plastic strain at the n-th unloading/reloading cycle, while $\varepsilon_{pl,n-1}$ denotes the plastic strain from the previous *(n-1)-th* cycle.

The subsequent paragraphs examine the models proposed for predicting the plastic strain and stress deterioration caused by repeated complete unloading/reloading cycles. Lam and Teng [10], for instance, presented a formulation for the increasing strain ratio, γ_n, which is discussed below.

$$\gamma_n = \begin{cases} 1, & 0 \leq \varepsilon_{ul,1} < 0.001 \\ 1 + 400(0.0212n - 0.12) \times (\varepsilon_{ul,1} - 0.001), & 0.001 \leq \varepsilon_{ul,1} < 0.0035 \\ 0.0212n + 0.88, & \varepsilon_{ul,1} \geq 0.0035 \end{cases} \tag{11}$$

They suggested that this equation is applicable for $2 \leq n \leq 5$ and when $n \geq 6$, $\gamma_n = 1$.

It should be noted that in the test data of Lam and Teng [10], only 3 unloading-reloading cycles were repeated at each prescribed envelope unloading strain. Thus equation 11 is obtained with two points. Therefore, for $n \geq 3$, the accuracy of this equation should be examined.

Ziaadiny and Abbasnia [14] illustrated that the average value of γ_n increases with the increase in the number of cycles (n). The following equation is proposed for the γ_n [14].

$$\gamma_n = \begin{cases} 0.950 & n = 2 \\ 0.00646n + 0.948 & 3 \leq n < 8 \\ 1 & n \geq 8 \end{cases} \tag{12}$$

Their study involved specimens subjected to up to 11 internal cycles, leading them to conclude that when $n \geq 8$, γ_n reaches approximately 1. This finding indicates that beyond eight cycles, the cumulative effect of additional cycles on the plastic strain of FRP-confined concrete prisms becomes negligible.

On the other hand, Yu et al. [13] evaluated Lam and Teng's earlier model and identified limitations in its accuracy. While Eq. (11) generally provided reliable predictions for cases where $n < 5$, it consistently overestimated the experimental results when $n \geq 6$. To address these discrepancies, Yu et al. proposed an alternative formulation for γ_n, as presented in the following section.

$$\gamma_n(n \geq 2) = \begin{cases} 1, & 0 \leq \varepsilon_{ul,1} < 0.001 \\ 1 + 32(\varepsilon_{ul,1} - 0.001) \times (n-1), & 0.001 \leq \varepsilon_{ul,1} < 0.0035 \\ 0.0212n + 0.88, & \varepsilon_{ul,1} \geq 0.0035 \end{cases} \tag{13}$$

The experimental results for γ_n and the model predictions are compared in Figure 3. This figure shows that the model proposed by Yu et al. has the best performance among the examined models. The only deficiency of this model is that for internal cycles with high "n" this model does not reach to $\gamma_n = 1$. The average value of experimental results shows that for $n \geq 8$, γ_n is almost near to 1 and the cumulative effect of repeated cycles on the plastic strain is negligible. As it is obvious from the figures, Ziaadiny and Abbasnia's model has relatively good predictions of average values of γ_n except for $n = 2$. Thus, the modified version of this model is proposed to predict γ_n.

$$\gamma_n = \begin{cases} 0.930 & n = 2 \\ 0.00646n + 0.948 & 3 \leq n < 8 \\ 1 & n \geq 8 \end{cases} \tag{14}$$

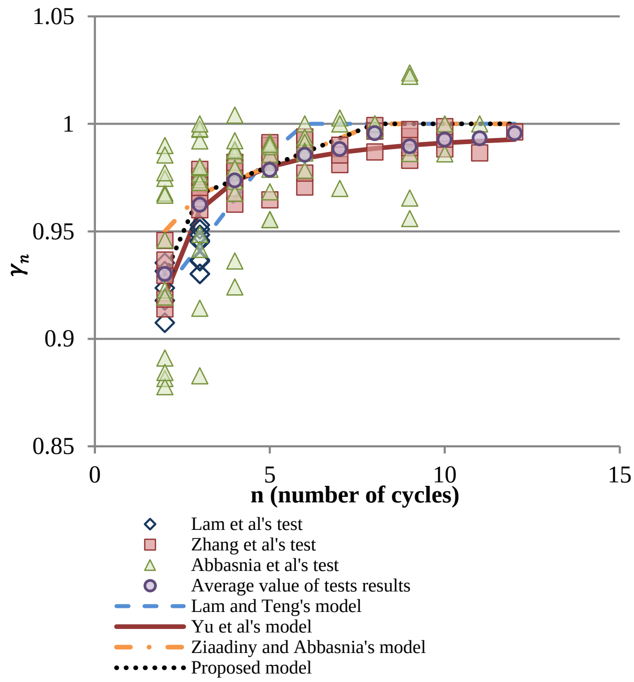

Fig. 3: Experimental results and model predictions for strain accumulation ratio γ_n versus cycle number n

5.2 Stress deterioration of repeated complete cycles

Sakai and Kawashima [25] defined the stress deterioration ratio for the *n-th* cycle to evaluate the degree of stress deterioration for the *n-th* unloading/reloading cycle, as follows:

$$\beta_n = \frac{f_{new,n}}{f_{new,n-1}} \tag{15}$$

Where $f_{new,1}$ is the new stress where the first reloading path reaches the $\varepsilon_{ul,1}$, and $f_{new,n}$is the new stress where the *n-th* reloading path reaches the $\varepsilon_{ul,1}$.

Lam and Teng [10] proposed strain deterioration ratio β_n as:

$$\beta_n = \begin{cases} 1, & 0 \leq \varepsilon_{ul,1} < 0.001 \\ 1 + 1000(0.013n - 0.075) \times (\varepsilon_{ul,1} - 0.001), & 0.001 \leq \varepsilon_{ul,1} < 0.002 \\ 0.013n + 0.925, & \varepsilon_{ul,1} \geq 0.002 \end{cases} \tag{16}$$

They demonstrated that this equation is applicable when $2 \leq n \leq 5$ and when $n \geq 6$, $\beta_n = 1$.

Similar to increasing strain ratio γ_n, the stress deterioration ratio β_n (Eq.16) is obtained with only two points, and for $n \geq 3$ the accuracy of this equation should be examined.

Yu et al. [13] showed that Lam and Teng's model for stress deterioration β_n provides reasonably accurate predictions when $n < 5$, but overestimates the test results when $n \geq 6$. They proposed β_n as:

$$\beta_n = \begin{cases} 1, & 0 \leq \varepsilon_{ul,1} < 0.001 \\ 1 + 80\dfrac{(\varepsilon_{ul,1} - 0.001)}{n}, & 0.001 \leq \varepsilon_{ul,1} < 0.0035 \\ \dfrac{-0.08}{n} + 1, & \varepsilon_{ul,1} \geq 0.0035 \end{cases} \tag{17}$$

Ziaadiny [26] demonstrated that the average value of β_n, similar to γ_n, increases as the number of cycles (n) grows. However, the rate of this increase diminishes notably when $n = 3$, indicating a reduction in the incremental impact of subsequent cycles. Furthermore, for $n > 8$, β_n stabilizes at approximately 1, suggesting that additional cycles beyond this threshold do not significantly contribute to further stress deterioration. Based on these observations, Ziaadiny proposed the following piecewise equations for β_n:

For $1 < n \leq 3$

$$\beta_n = \begin{cases} 1, & 0 \leq \varepsilon_{ul,1} < 0.001 \\ (12.8n - 52.8) \times (\varepsilon_{ul,1} - 0.001) + 1, & 0.001 \leq \varepsilon_{ul,1} < 0.0035 \\ 0.032n + 0.868, & \varepsilon_{ul,1} \geq 0.0035 \end{cases} \tag{18-a}$$

For $4 \leq n < 8$

$$\beta_n = \begin{cases} 1, & 0 \leq \varepsilon_{ul,1} < 0.001 \\ (2.88n - 23.04) \times (\varepsilon_{ul,1} - 0.001) + 1, & 0.001 \leq \varepsilon_{ul,1} < 0.0035 \\ 0.0072n + 0.9424, & \varepsilon_{ul,1} \geq 0.0035 \end{cases} \tag{18-b}$$

And for $n \geq 8$,

$$\beta_n = 1 \tag{18-c}$$

Figure 4 compares the experimental stress deterioration ratio β_n with predictions from various models. This figure shows that the model proposed by Lam and Teng [10] has relatively good results for $2 \leq n \leq 5$. Yu et al.'s model [13] has a close prediction of the average values of experimental results and this model can be used for the prediction of stress deterioration of internal cycles. However, for $n \geq 8$, $\beta_n = 1$ can be taken thus the proposed model which is a modified version of Ziaadiny and Abbasnia's model can be used for stress deterioration of internal cycles β_n. It should be mentioned that in the modified version all part of the model is similar to Ziaadiny and Abbasnia's model except for $1 < n \leq 3$, β_n is proposed as:

$$\beta_n = \begin{cases} 1, & 0 \leq \varepsilon_{ul,1} < 0.001 \\ (12.8n - 52.8) \times (\varepsilon_{ul,1} - 0.001) + 1, & 0.001 \leq \varepsilon_{ul,1} < 0.0035 \\ 0.027n + 0.883, & \varepsilon_{ul,1} \geq 0.0035 \end{cases} \quad (19)$$

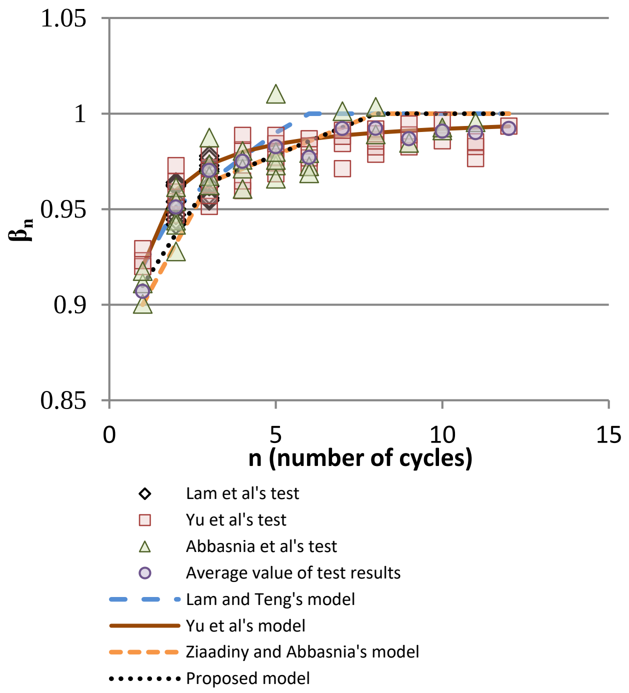

Fig. 4: Experimental results and model predictions for stress deterioration ratio β_n versus cycle number n

6. Partial unloading and partial reloading cycles

Unlike the complete cycles, loading or unloading paths can be incomplete. When the unloading path from the envelope curve terminates before reaching zero stress, this case is named partial unloading. When the reloading path terminates before reaching the envelope unloading strain, this case is called a partial reloading cycle. Sakai and Kawashima [25] defined partial unloading ratio β_{UL} and partial reloading ratio γ_{RL} to examine the effects of partial cycles:

$$\beta_{UL} = \frac{f_{ul,1} - f_{rl}}{f_{ul,1}} \quad (20)$$

$$\gamma_{RL} = \frac{\varepsilon_{ul,in} - \varepsilon_{pl,1}}{\varepsilon_{ul} - \varepsilon_{pl,1}} \quad (21)$$

In the following subsections, existing formulations for partial cycles in FRP-confined concrete are presented and discussed.

Shao et al. [8] proposed that unloading from any arbitrary point on the reloading path follows a trajectory similar to the primary unloading branch observed in complete cycles. This suggestion implies that partial reloading cycles do not contribute to an increase in plastic strain. Similarly, they indicated that reloading from any arbitrary point on the unloading path follows a path resembling the primary reloading branch of complete cycles, meaning these cycles do not lead to stress deterioration.

On the other hand, Lam and Teng [10] argued that partial cycles have a cumulative effect on both plastic strain and stress deterioration. According to their model, when the partial reloading strain ratio γ_{RL} exceeds 0.7, partial reloading cycles begin to affect both plastic strain and stress deterioration. Similarly, they suggested that when the partial unloading ratio β_{UL} exceeds 0.7, partial unloading cycles contribute to stress deterioration. Yu et al. [13] adopted a similar approach to that of Lam and Teng [10] in modeling the effects of partial unloading and partial reloading cycles.

Abbasnia and Ziaadiny [14] demonstrated that partial reloading cycles do not lead to stress deterioration in specimens unless γ_{RL} exceeds 0.8, at which point partial reloading begins to influence the accumulation of plastic strain. Additionally, they observed that complete unloading cycles generally result in greater stress deterioration compared to partial unloading cycles. They further suggested that partial unloading cycles cause stress deterioration when β_{UL} exceeds 0.7.

It should be mentioned that Lam and Teng [10] and Yu et al. [13] did not have specimens with partial cycles in their test database, but Ziaadiny and Abbasnia [14] had specimens with partial unloading and partial reloading cycles. Thus, Ziaadiny and Abbasnia's formulation for partial cycles is more reliable than other models.

7. Models for unloading path

7.1 Shao et al.'s model [8]

Shao et al. [8] proposed that the unloading curve is influenced by the unloading stress level $f_{ul,1}$, and its relative position to the bend point on the envelope curve. According to their model, when unloading occurs before reaching the bend point on the envelope curve, the unloading path follows a linear trajectory that returns to the origin. Conversely, when unloading begins above the bend point, the path becomes curvilinear and terminates at a residual or plastic strain ε_{pl} with a zero slope. The unloading path is mathematically expressed by the following equation:

$$f_c = \frac{(1-x)^{n1}}{(1-kx)^{n2}} f_{ul,1} \tag{22}$$

In this equation, x represents the normalized strain along the unloading branch, which is defined as:

$$x = \frac{\varepsilon_c - \varepsilon_{ul,1}}{\varepsilon_{pl} - \varepsilon_{ul,1}} \qquad 0 < x < 1 \tag{23}$$

And n_1, n_2, k are the shape parameters.

7.2 Lam and Teng's model [10]

Lam and Teng [10] proposed a polynomial equation to represent the unloading paths of the cyclic stress-strain of FRP-confined concrete:

$$f_c = a{\varepsilon_c}^{\eta} + b\varepsilon_c + c \tag{24-1}$$

$$a = \frac{f_{ul} - E_{un,0}(\varepsilon_{ul} - \varepsilon_{pl})}{{\varepsilon_{ul}}^{\eta} - {\varepsilon_{pl}}^{\eta} - \eta{\varepsilon_{pl}}^{\eta-1}(\varepsilon_{ul} - \varepsilon_{pl})} \tag{24-2}$$

$$b = E_{ul,0} - \eta{\varepsilon_{pl}}^{\eta-1}a \tag{24-3}$$

$$c = -a{\varepsilon_{pl}}^{\eta} - b\varepsilon_{pl} \tag{24-4}$$

$$\eta = 350\varepsilon_{ul} + 3 \tag{24-5}$$

$$E_{ul,0} = min\begin{cases} \dfrac{0.5f'_{co}}{\varepsilon_{ul}} \\ \dfrac{f_{ul}}{\varepsilon_{ul} - \varepsilon_{pl}} \end{cases} \tag{24-6}$$

7.3 Yu et al.'s model [13]

Yu et al. adopted Lam and Teng's model for the unloading path. They demonstrated that Lam and Teng's model inaccurately represents the unloading path of higher-strength concrete. Thus, they modified the parameter η to consider the effect of concrete strength:

$$\eta = \frac{40(350\varepsilon_{ul} + 3)}{f'_{co}} \tag{25}$$

7.4 Ziaadiny and Abbasnia's model [14]

Ziaadiny and Abbasnia [14] demonstrated that the envelope unloading paths of FRP-confined prisms consist of two distinct segments. In the initial phase, the axial strain increases until it reaches $\varepsilon_{ul,max}$. Following this, the concrete follows a nonlinear path down to zero stress. To model the second segment, the normalized strain is first defined as follows:

$$x = \frac{\varepsilon_c - \varepsilon_{pl,1}}{\varepsilon_{ul,max} - \varepsilon_{pl,1}} \tag{26}$$

The second segment of the envelope unloading path is modeled using the following formulation:

$$f_c = f_{ul,max}x^{\mu} \tag{27}$$

Where μ is a constant that controls the curvature of the nonlinear part of the unloading path:

$$\begin{aligned}\mu &= [-2.073f'_{co} + 236.7]\varepsilon_{ul,1} \\ &+ [-0.024f'_{co} + 2.398]\end{aligned} \tag{28}$$

Figure 5 depicts the performance of models in predicting the unloading path. This figure demonstrates that the shape of unloading path in all models is well-predicted. However, Lam and Teng's model and Yu et al.'s model did not account for the increase of the unloading strain during the early stages of envelope unloading paths, the unloading path of their models do not align with the experimental data. (See Figure 5). Also, it is evident from these figures that the slope of the unloading path does not terminate at a zero slope; thus, Shao et al.'s model fails to accurately predict the unloading path and was excluded from the comparison.

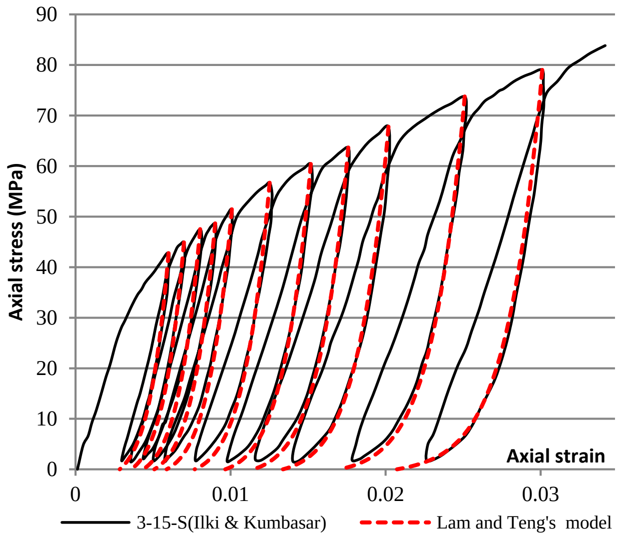

a) 3-15-S (Ilki and Kumbasar) – Lam and Teng's model

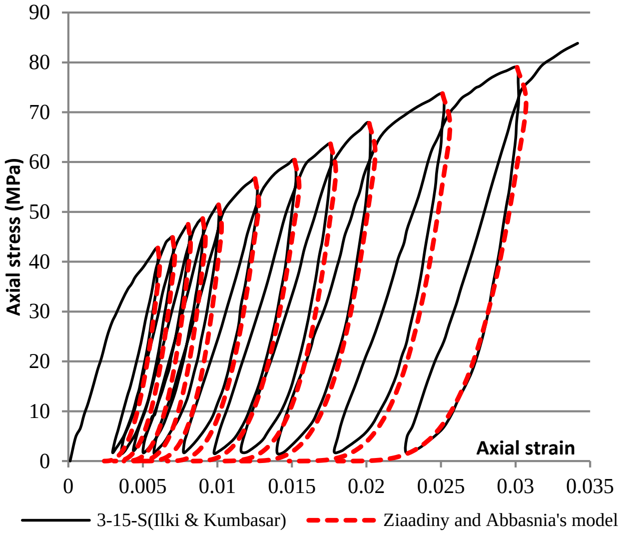

b) 3-15-S (Ilki and Kumbasar) – Ziaadiny and Abbasnia's model

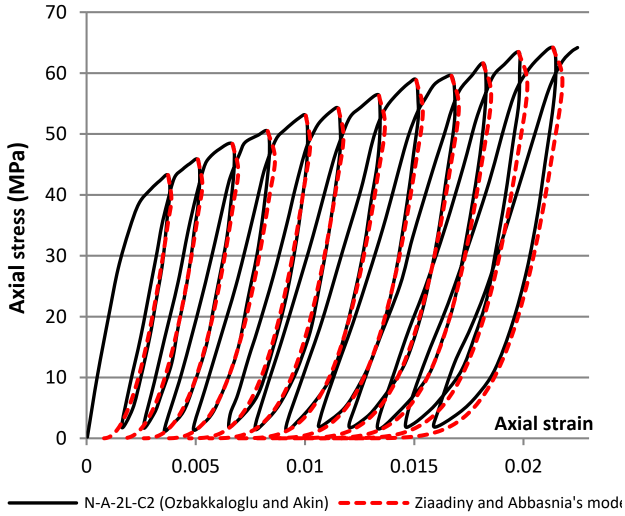

e) N-A-2L-C2 (Ozbakkaloglu and Akin) – Ziaadiny and Abbasnia's model

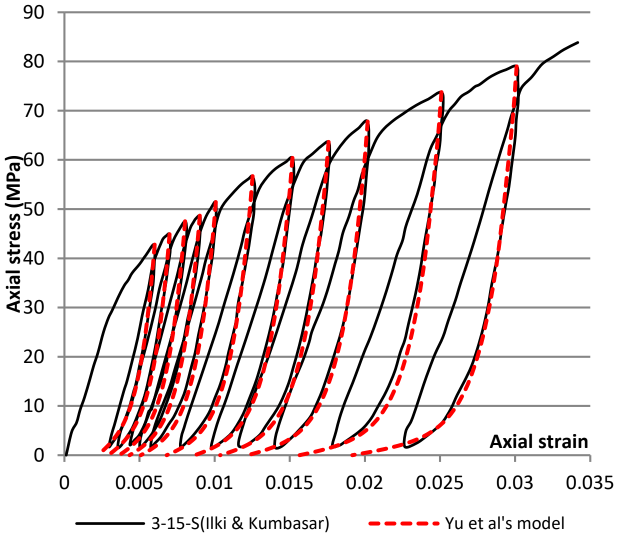

c) 3-15-S (Ilki and Kumbasar) – Yu et al.'s model

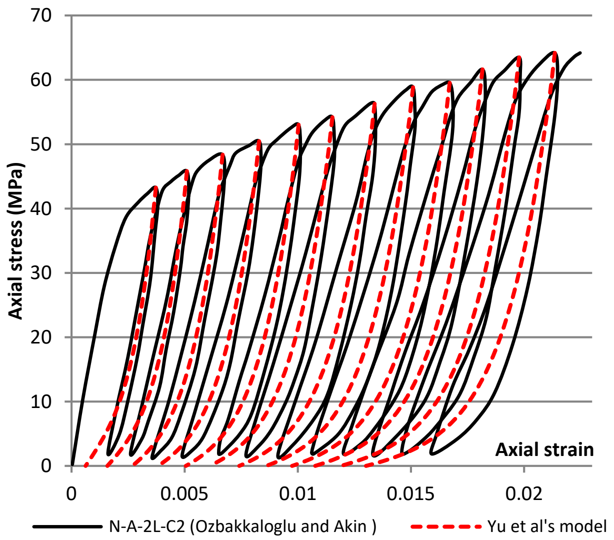

f) N-A-2L-C2 (Ozbakkaloglu and Akin) – Yu et al.'s model

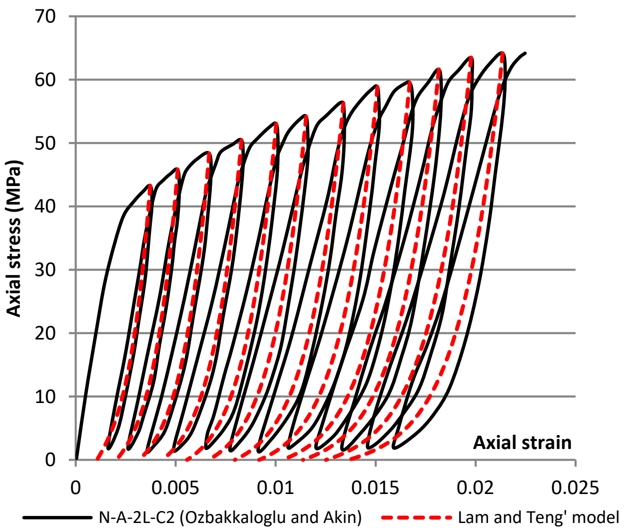

d) N-A-2L-C2 (Ozbakkaloglu and Akin) – Lam and Teng's model

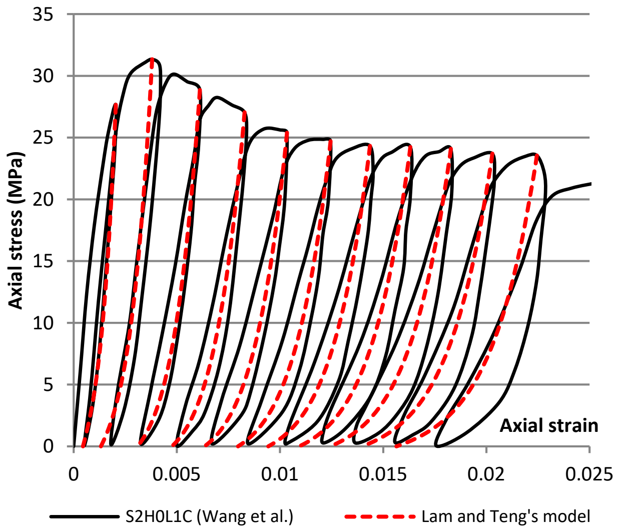

g) S2H0L1C (Wang et al.) – Lam and Teng's model

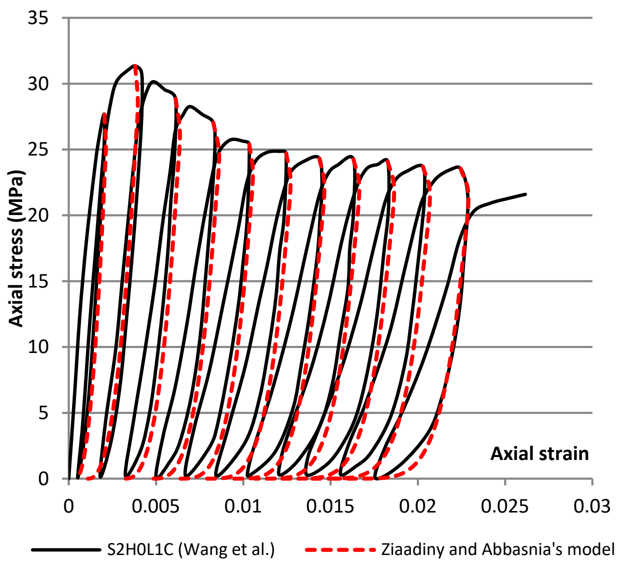

h) S2H0L1C (Wang et al.) – Ziaadiny and Abbasnia's model

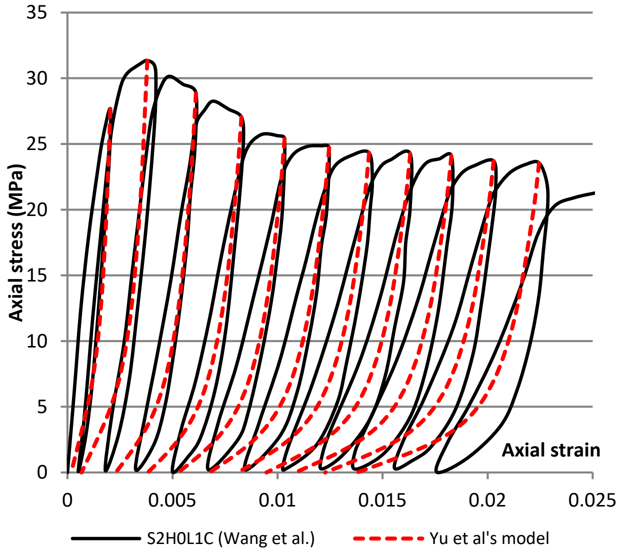

i) S2H0L1C (Wang et al.) – Yu et al.'s model

Fig. 5: Unloading path predictions: Model performance vs. experimental data

8. Models for reloading path

8.1 Shao et al.'s model [8]

In Shao et al.'s [8] model, the entire reloading path is modeled as a linear curve. They proposed that the reloading path before the bend point of the envelope curve has no stress deterioration and the reloading path reaches the first envelope unloading point. Above the bend point, stress deterioration occurs; accordingly, the reloading branch is constructed between the point of plastic strain (ε_{pl}, 0) and the new stress level (ε_{ul}, f_{new}), and then extended with the same slope until it rejoins the envelope curve.

8.2 Lam and Teng's model [10]

The proposed reloading path in Lam and Teng's model consists of a linear first portion from the reloading strain point (ε_{re}, f_{re}) to the point (ε_{ref}, f_{new}), and a parabolic portion for the remaining part, until it meets the envelope curve. The linear portion of the reloading path is defined as:

$$f_c = f_{re} + E_{re}(\varepsilon_c - \varepsilon_{re}) \tag{29}$$

Where E_{re} is the slope of the linear portion:

$$E_{re} = (f_{new} - f_{re})/(\varepsilon_{ref} - \varepsilon_{re}) \tag{30}$$

The parabolic portion is defined as:

$$f_c = A\varepsilon_c^2 + B\varepsilon_c + C \tag{31}$$

Where, A, B, and C are constants to be determined as:

$$A = \frac{(E_c - E_2)^2(E_{re}\varepsilon_{ref} - f_{new}) + (E_c - E_{re})^2 f'_{co}}{4(f_{new} - E_c\varepsilon_{ref})f'_{co} + (E_c - E_2)^2\varepsilon_{ref}^2} \tag{32-1}$$

$$B = E_{re} - 2A\varepsilon_{ref} \tag{32-2}$$

$$C = f_{new} - A\varepsilon_{ref}^2 - B\varepsilon_{ref} \tag{32-3}$$

For more details see ref [10].

8.3. Yu et al.'s model [13]:

Yu et al. [13] adopted the Lam and Teng's model for the reloading path. They used their new expression for f_{new}, thus, the slope of the linear part of the reloading path is different from that of Lam and Teng's model.

8.4. Ziaadiny and Abbasnia's model [14]:

Ziaadiny and Abbasnia [14] demonstrated that the reloading paths of FRP-confined prisms are nonlinear, with the degree of nonlinearity increasing as the envelope unloading strain grows. Similar to the unloading path, the curvature of the reloading path decreases with higher concrete strength. They proposed a two-part model for the complete reloading path. The initial segment, between points "c" and "d" (or "f" and "g"), is modeled in a manner similar to the nonlinear portion of the unloading path. The second segment, from point "d" (or "g") to the envelope returning point (point "e"), is represented as a linear function.

To model the first part, the normalized strain is initially defined as follows:

$$x = \frac{\varepsilon_c - \varepsilon_{pl,n}}{\varepsilon_{ul,max} - \varepsilon_{pl,n}} \tag{33}$$

And the first part of the complete reloading path is modeled as follows:

$$f_c = f_{new,n} x^{\eta} \tag{34}$$

Where η is the constant to be determined and when this constant increases, the curvature of the reloading path increases.

$$\eta = \begin{cases} [-1.706 f'_{co} + 92.56]\varepsilon_{ul,1} + [-0.003 f'_{co} + 1.088], & f'_{co} \leq 55MPa \\ 0.9, & f'_{co} > 55MPa \end{cases} \tag{35}$$

If reloading begins before the unloading path reaches zero stress (partial unloading), the reloading path is simplified and represented as a linear function connecting two points, “i” and “g” (refer to Figure 6):

$$f_c = \left[\frac{f_{new,n} - f_{re}}{\varepsilon_{ul,max} - \varepsilon_{re}}\right](\varepsilon_c - \varepsilon_{re}) + f_{re} \tag{36}$$

The second part of the reloading path, starting from point "d" (or "g") and extending to the envelope returning point "e," is idealized as a linear function. However, this linear section has a reduced slope compared to the slope of the first part at $x = 1$ (refer to Figure 6). If the slope of this second part is k times the slope of Equation (22) at $x = 1$, then the linear function for this portion of the reloading path can be expressed as follows:

$$f_c = (k\eta f_{new,n})x + f_{new,n}(1 - k\eta) \tag{37}$$

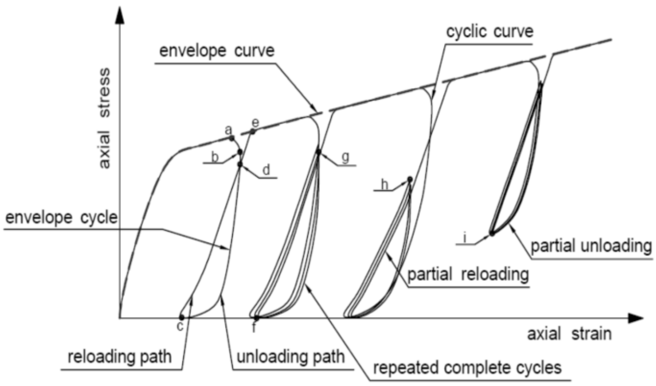

Fig. 6: Different parts and basic points of the cyclic stress-strain curve

It is concluded from the experimental results that the best value for coefficient “k” is equal to 0.45.

Figure 7 depicts the performance of models in predicting reloading path. These figures demonstrate that the reloading path in all models is well predicted. However, Lam and Teng’s model and Yu et al.'s model did not consider the increase of unloading strain in the early stage of envelope unloading paths, thus in some specimens reloading path of their models does not match experimental data. (See Figure 7).

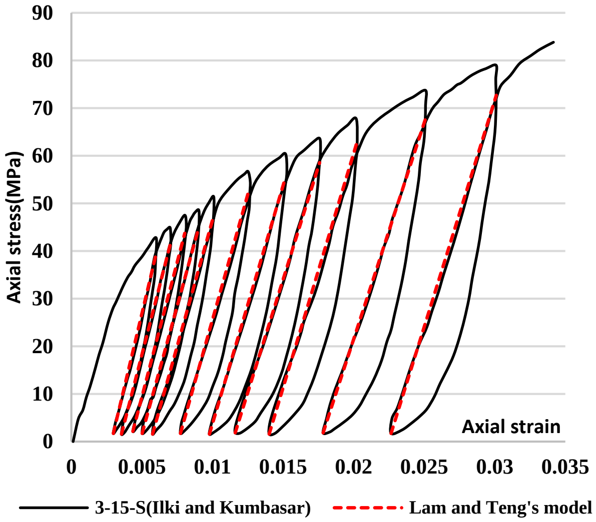

a) 3-15-S (Ilki and Kumbasar) – Lam and Teng's model

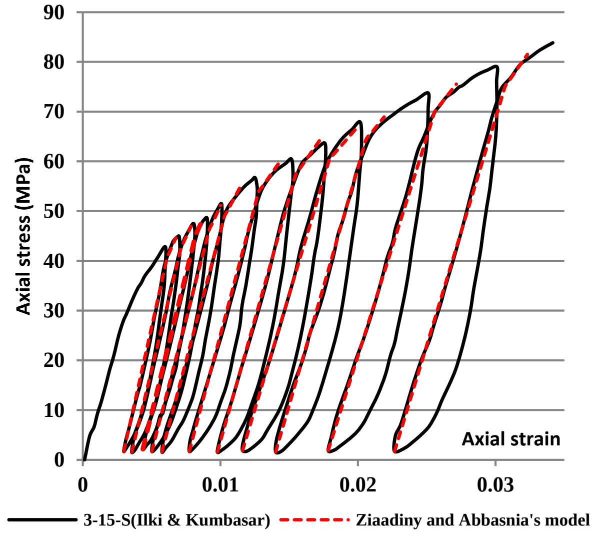

b) 3-15-S (Ilki and Kumbasar) – Ziaadiny and Abbasnia's model

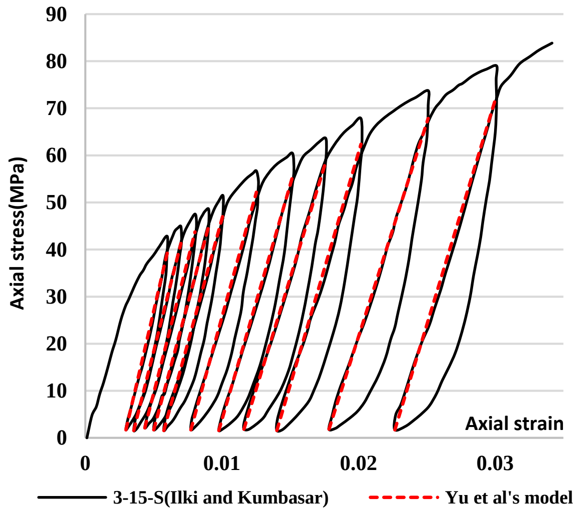

c) 3-15-S (Ilki and Kumbasar) – Yu et al.'s model

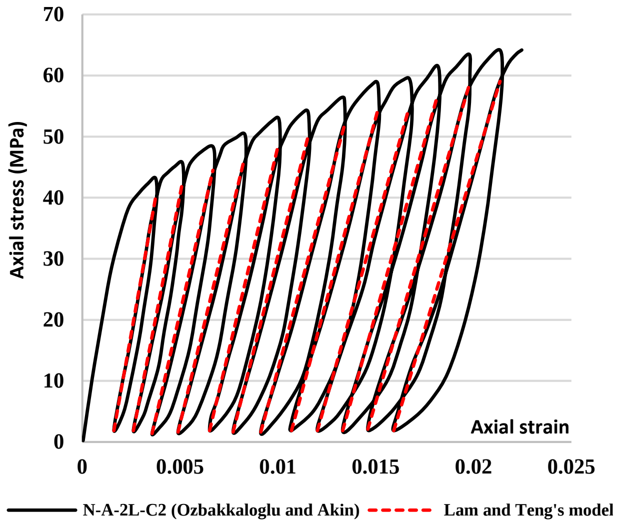

d) N-A-2L-C2 (Ozbakkaloglu and Akin) – Lam and Teng's model

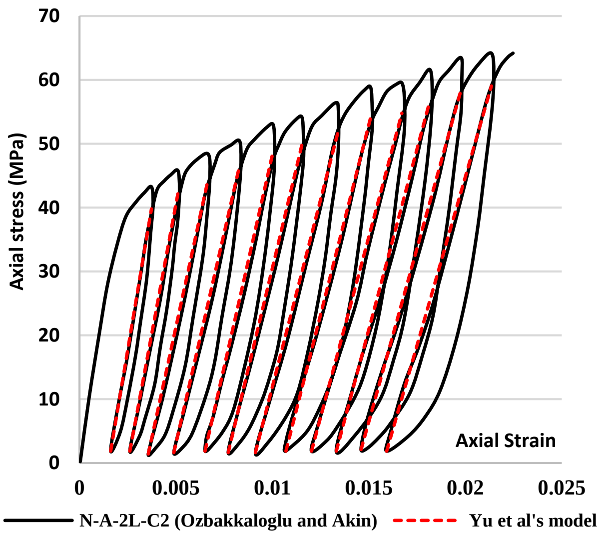

e) N-A-2L-C2 (Ozbakkaloglu and Akin) – Yu et al.'s model

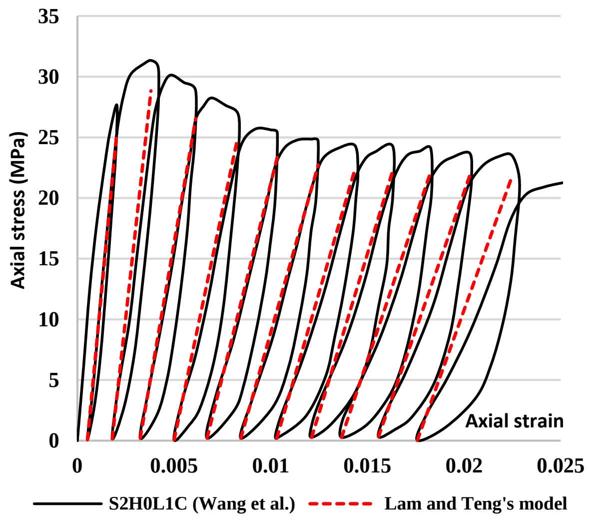

f) S2H0L1C (Wang et al.) – Lam and Teng's model

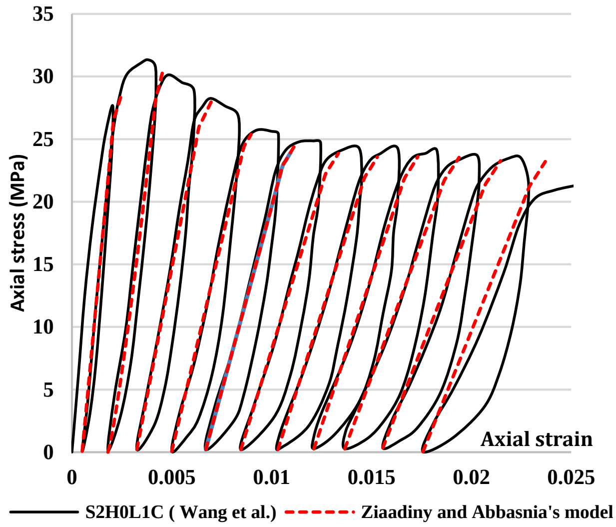

g) S2H0L1C (Wang et al.) – Ziaadiny and Abbasnia's model

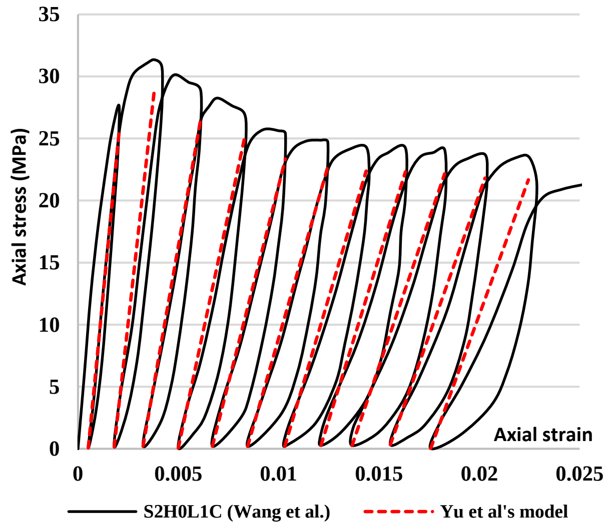

h) S2H0L1C (Wang et al.) – Yu et al.'s model

Fig. 7: Reloading path predictions: Model performance vs. experimental data

9. Conclusions

In this paper, a critical review of existing cyclic stress–strain models for FRP-confined concrete is provided, and certain modifications are proposed to improve the accuracy and applicability of the models examined. Based on the analyses and results of this study, the following conclusions can be made:

1. **Monotonic Stress-Strain Models**: Existing models for the monotonic stress-strain behavior of FRP-confined concrete prisms are highly accurate and can be effectively applied to model the envelope curve of cyclic stress-strain behavior. These models offer reliable predictions for the overall response of FRP-confined concrete under monotonic loading conditions, which can be extended to cyclic scenarios.

2. **Accuracy of Lam and Teng's Model**: Lam and Teng's cyclic stress-strain model [10] provides more accurate predictions for the plastic strain behavior during unloading and reloading cycles. The model effectively captures the key characteristics of the cyclic behavior, making it a valuable tool for assessing the performance of FRP-confined concrete under cyclic loading.
3. **Stress Deterioration Ratio**: From the experimental results, the average value of the stress deterioration ratio β_1 was found to be 0.907 for unloading strains greater than 0.0035. Based on these findings, it is recommended that for $\varepsilon_{ul,env} \geq 0.0035$, the stress deterioration ratio β_1 should be taken as 0.91 for more accurate predictions.
4. **Modified Model for Repeated Complete Cycles**: The modified version of Abbasnia and Ziaadiny's model is effective for predicting the plastic strain and stress deterioration in repeated complete unloading/reloading cycles. This updated model addresses the observed discrepancies in the original formulation and improves the accuracy of predictions under multiple-cycle conditions.
5. **Unloading and Reloading Paths**: The unloading and reloading paths of the cyclic stress-strain behavior can be accurately predicted using Abbasnia and Ziaadiny's model. For partial unloading/reloading cycles, the adopted empirical thresholds (e.g., partial reloading ratio) show good agreement with available data, though their theoretical basis requires further investigation, particularly for non-circular sections and high confinement scenarios. In contrast, Lam and Teng's model, as well as Yu et al.'s model, do not account for the increase in unloading strain during the early stages of the envelope unloading path. As a result, the unloading path predictions from these models do not align well with experimental data. This limitation highlights the importance of incorporating the early-stage behavior of unloading strain for more accurate modeling.

Finally, while the proposed modifications demonstrate improved agreement with available experimental results, their robustness across a wider range of practical scenarios requires further investigation. Future studies should prioritize expanded datasets and probabilistic analyses to quantify model uncertainties under diverse conditions, with particular attention to nonlinear effects in high-strain regimes and confinement-dependent path behaviors.

References

[1] Y. Moodi, "Providing Models of the Compressive Strength of Square and Rectangular (S/R) Concrete Confined Using Genetic Programming," *Numerical Methods in Civil Engineering,* vol. 9, no. 3, pp. 16-27, 2025, doi: https://doi.org/10.61186/NMCE.2312.1040.

[2] A. Ilki and N. Kumbasar, "Behavior of damaged and undamaged concrete strengthened by carbon fiber composite sheets," *Structural Engineering and Mechanics,* vol. 13, no. 1, pp. 75-90, 2002, doi: https://doi.org/10.12989/sem.2002.13.1.075.

[3] T. Ozbakkaloglu and E. Akin, "Behavior of FRP-Confined Normal- and High-Strength Concrete under Cyclic Axial Compression," *Journal of Composites for Construction,* vol. 16, no. 4, pp. 451-463, 2012, doi: https://doi.org/10.1061/(ASCE)CC.1943-5614.0000273.

[4] V. Valdmanis, L. De Lorenzis, T. Rousakis, and R. Tepfers, "Behaviour and capacity of CFRP-confined concrete cylinders subjected to monotonic and cyclic axial compressive load," *Structural Concrete,* vol. 8, no. 4, pp. 187-200, 2007, doi: https://doi.org/10.1680/stco.2007.8.4.187.

[5] M. R. Shokrzadeh and F. Nateghi-Alahi, "Evaluation of hybrid NSM-CFRP technical bars and FRP sheets for seismic rehabilitation of a concrete bridge pier," *Bridge Structures,* vol. 18, no. 3-4, pp. 75-88, 2023, doi: https://doi.org/10.3233/brs-290180.

[6] M. r. Shokrzadeh, M. Sharifi, and F. Nateghi Alahe, "Seismic Retrofitting of Concrete Beam-Column Connections: Numerical study FRP Strip and NSM Technique," *Journal of Seismology and Earthquake Engineering,* vol. 26, no. 3, pp. 25-40, 2024, doi: https://doi.org/10.48303/jsee.2024.2031006.1099.

[7] M. R. Shokrzadeh, A. Aziminejad, and A. S. Moghaddam, "Evaluation of various FRP strengthening configurations for RC beam-column joints," *Bridge Structures,* vol. 20, no. 1-2, pp. 71-91, 2024, doi: https://doi.org/10.3233/brs-240223.

[8] Y. Shao, Z. Zhu, and A. Mirmiran, "Cyclic modeling of FRP-confined concrete with improved ductility," *Cement and Concrete Composites,* vol. 28, no. 10, pp. 959-968, 2006, doi: https://doi.org/10.1016/j.cemconcomp.2006.07.009.

[9] L. Lam, J. G. Teng, C. H. Cheung, and Y. Xiao, "FRP-confined concrete under axial cyclic compression," *Cement and Concrete Composites,* vol. 28, no. 10, pp. 949-958, 2006, doi: https://doi.org/10.1016/j.cemconcomp.2006.07.007.

[10] L. Lam and J. G. Teng, "Stress–strain model for FRP-confined concrete under cyclic axial compression," *Engineering Structures,* vol. 31, no. 2, pp. 308-321, 2009, doi: https://doi.org/10.1016/j.engstruct.2008.08.014.

[11] Z. Wang, D. Wang, S. T. Smith, and D. Lu, "Experimental testing and analytical modeling of CFRP-confined large circular RC columns subjected to cyclic axial compression," *Engineering Structures,* vol. 40, pp. 64-74, 2012, doi: https://doi.org/10.1016/j.engstruct.2012.01.004.

[12] Z. Wang, D. Wang, S. T. Smith, and D. Lu, "CFRP-Confined Square RC Columns. II: Cyclic Axial Compression Stress-Strain Model," *Journal of Composites for Construction,* vol. 16, no. 2, pp. 161-170, 2012, doi: https://doi.org/10.1061/(asce)cc.1943-5614.0000246.

[13] T. Yu, B. Zhang, and J. G. Teng, "Unified cyclic stress–strain model for normal and high strength concrete confined with FRP," *Engineering Structures,* vol. 102, pp. 189-201, 2015, doi: https://doi.org/10.1016/j.engstruct.2015.08.014.

[14] H. Ziaadiny and R. Abbasnia, "Unified cyclic stress-strain model for FRP-confined concrete circular, square and rectangular prisms," *Structural Concrete,* vol. 17, no. 2, pp. 220-234, 2016, doi: https://doi.org/10.1002/suco.201500128.

[15] M. Samaan, A. Mirmiran, and M. Shahawy, "Model of Concrete Confined by Fiber Composites," *Journal of Structural Engineering,* vol. 124, no. 9, pp. 1025-1031, 1998, doi: https://doi.org/10.1061/(asce)0733-9445(1998)124:9(1025).

[16] L. Lam and J. G. Teng, "Design-oriented stress–strain model for FRP-confined concrete," *Construction and Building Materials,* vol. 17, no. 6-7, pp. 471-489, 2003, doi: https://doi.org/10.1016/s0950-0618(03)00045-x.

[17] R. Abbasnia, R. Ahmadi, and H. Ziaadiny, "Effect of confinement level, aspect ratio and concrete strength on the cyclic stress–strain behavior of FRP-confined concrete prisms," *Composites Part B: Engineering,* vol. 43, no. 2, pp. 825-831, 2012, doi: https://doi.org/10.1016/j.compositesb.2011.11.008.

[18] R. Abbasnia, F. Hosseinpour, M. Rostamian, and H. Ziaadiny, "Effect of corner radius on stress–strain behavior of FRP confined prisms under axial cyclic compression," *Engineering Structures,* vol. 40, pp. 529-535, 2012, doi: https://doi.org/10.1016/j.engstruct.2012.03.020.

[19] R. Abbasnia and H. Ziaadiny, "Behavior of concrete prisms confined with FRP composites under axial cyclic compression," *Engineering Structures,* vol. 32, no. 3, pp. 648-655, 2010, doi: https://doi.org/10.1016/j.engstruct.2009.11.011.

[20] R. Abbasnia and H. Ziaadiny, "Behavior of FRP confined rectangular prisms under cyclic loading," MSc., Department of Civil Engineering, Iran University of Science and Technology, Tehran, Iran, 2013.

[21] R. Abbasnia and H. Ziaadiny, "Behavior and modeling of FRP confined concrete rectangular prisms under axial cyclic compression," PhD, Department of Civil Engineering, Iran University of Science and Technology, Tehran, Iran, 2013.

[22] H. Ziaadiny, R. Abbaszadeh, V. Razavinasab, and S. M. Elhamnike, "Behaviour of preloaded concrete cylinders confined by fibre-reinforced polymer composites," *Proceedings of the Institution of Civil Engineers - Structures and Buildings,* vol. 175, no. 9, pp. 697-708, 2022, doi: https://doi.org/10.1680/jstbu.20.00001.

[23] R. Abbasnia and H. Ziaadiny, "Experimental investigation and strength modeling of CFRP-confined concrete rectangular prisms under axial monotonic compression," *Materials and Structures,* vol. 48, no. 1-2, pp. 485-500, 2013, doi: https://doi.org/10.1617/s11527-013-0198-y.

[24] J. G. Teng, T. Jiang, L. Lam, and Y. Z. Luo, "Refinement of a Design-Oriented Stress–Strain Model for FRP-Confined Concrete," *Journal of Composites for Construction,* vol. 13, no. 4, pp. 269-278, 2009, doi: https://doi.org/10.1061/(asce)cc.1943-5614.0000012.

[25] J. Sakai and K. Kawashima, "Unloading and Reloading Stress–Strain Model for Confined Concrete," *Journal of Structural Engineering,* vol. 132, no. 1, pp. 112-122, 2006, doi: https://doi.org/10.1061/(asce)0733-9445(2006)132:1(112).

[26] H. Ziaadiny, "Plastic strain and stress deterioration of FRP-confined concrete prisms under axial cyclic compression," *Materials and Structures,* vol. 49, no. 4, pp. 1157-1164, 2015, doi: https://doi.org/10.1617/s11527-015-0565-y.